Flow Measurement and Instrumentation 82 (2021) 102058

Contents lists available at ScienceDirect

Flow Measurement and Instrumentation

journal homepage: www.elsevier.com/locate/flowmeasinst

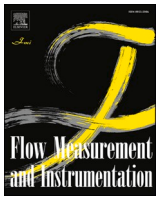

Laminar flowmeter for mechanical ventilator: Manufacturing challenge of Covid-19 pandemic

Jaafar Alsalaet, Basil Sh. Munahi, Raheem Al-Sabur, Mohammed Al-Saad, Abdulbaki K. Ali, Abdulbaseer Shari B, Hayder Ali Fadhil, Rafil M. Laftah, Muneer Ismael *

University of Basrah, Engineering College, Basrah, 61004, Iraq

ARTICLE INFO

Keywords:
Laminar flowmeter
Fleisch pneumotachograph
Ventilator
3D printing

ABSTRACT

The rapid and sudden attack of the covid-19 pandemic has emerged the urgent need for pulmonary resuscitation devices (ventilators). The airflow sensor is a main element in the ventilator. Sensing very low airflow rates is an essential requirement to meet the least significant bit of the analogue to digital converter included in the ventilator. This short communication describes the fabrication and test of five flow sensors using basic and the 3D printing techniques to overcome the severe challenge arising from the pandemic under strict quarantine. The principle of these five flow sensors is based on Fleisch pneumotachograph technology, which creates a pseudo-laminar flow within a bundle of capillary tubes. Amongst the five tested sensors, those fabricated by 3D printing technique were the most accurate and reliable. Results show that the 3D printed sensor of 33 trapezoidal capillary tubes and displaced pressure taps meet the requirement of sensing flowrates with less resistance to patient at exhalation and more linearity figure. The experimental data were correlated using a sophisticated MMF correlation with an R-squared factor of 0.9999 and a percentage error of 1.68%.

1. Introduction

Flow measurement is one of the most important processes in an artificial ventilator used to provide respiratory function when lung function is hindered for illness problems or when patients are subjected to general anesthesia. The functions of the flowmeter in such process are to monitor the airflow rate in expiration and inspiration and to integrate the flow to obtain the tidal volume provided to the patient. Without accurate continuous flow monitoring, volutrauma and barotrauma can injure the lung [1]. As such, the flowmeter should be selected or designed very carefully. As cited in Miller [2], more than 100 different flowmeters are available up to the mid of 1970s for different engineering and industrial applications. Therefore, the selection of a suitable flowmeter is a very critical decision. In mechanical ventilators (MVs), the selection of flowmeter is less confusing because the strict demands of medical applications limit the availability of the accepted flowmeter. The main demands of MVs are accuracy (even for low flow rate); stability (where the cyclic calibration is not permissible); sterilizable (if not replaceable); low-pressure drop (to avoid extra resistance in expiration); insensitive to moisture and secretions accumulation; insensitive to pulsative flow and interested in the measurement of gas flow and control of that gas flow. However, the compliance nature of the airway and the lung add more difficulties to the task of the flowmeter [3]. Undergoing covid-19 pandemic, the urgent need for artificial breathing devices, and the strict quarantine made the acquiring of MVs very difficult, if not impossible. Therefore, the collaborators of this paper have responded to the demand for local manufacturing of MVs where the flowmeter is a crucial sensor that cannot be averted.

A review of flowmeter used in MVs has revealed five different flowmeters working of different principles these are laminar flowmeter, variable area orifice flowmeter, hot wire flowmeter, ultrasonic flowmeter and the recently proposed flowmeter based on flexible membrane and fiber-optic sensing. It is worthy to review the characteristics of these flowmeters and then one can select the suitable type according to plausible reasons.

1.1. Laminar flowmeter (LM)

From its name, this type senses the pressure difference across a soft restriction made by a bundle of capillary tubes banded (or drilled) inside the main pipe (Fig. 1 (a)) with upstream and downstream pressure taps under laminar flow conditions. In this design, the flowmeter is well

* Corresponding author.
E-mail address: muneer.ismael@uobasrah.edu.iq (M. Ismael).

https://doi.org/10.1016/j.flowmeasinst.2021.102058
Received 6 February 2021; Received in revised form 13 September 2021; Accepted 27 September 2021
Available online 1 October 2021

known as Fleisch pneumotachograph which used in pulmonary research since 1950 [4,5]. The capillary tubes serve in; smoothing the flow; breaks down eddies in the flow and suppresses pulsative flow. It experiences the collection of the condensed water vapor which disturbs the sensitivity of the flowmeter, thus it is usually provided with a heating element to remove the condensed vapor. This adds some complexity and additional cost. As a modified version, Lilly [4] proposed a fine mesh (400 wire meshed in screen) to generate flow resistance (Fig. 1 (a)). The problem of the condensed vapor was treated by adding two lower screens on either side. However, this problem was not completely removed [6].

1.2. Orifice flowmeter

A sudden constriction is installed in the pipe to generate significant pressure changes. The constriction is made by inserting a plate with a central hole of diameter *d*. Orifice flowmeter is easy in construction and not expensive. It should be asserted that the flowmeter sensitivity is equivalent to the resistance imparted by the flowmeter; hence the nonlinear relation connecting input (flow rate) and output (pressure difference) limits the range of accuracy. Moreover, owing to the secondary eddies formed behind the constriction, the orifice flowmeter experience an overestimation of the pulsative flow. As such, the orifice flowmeter in its classical form (constant area) has the biggest limitation in ventilators [7].

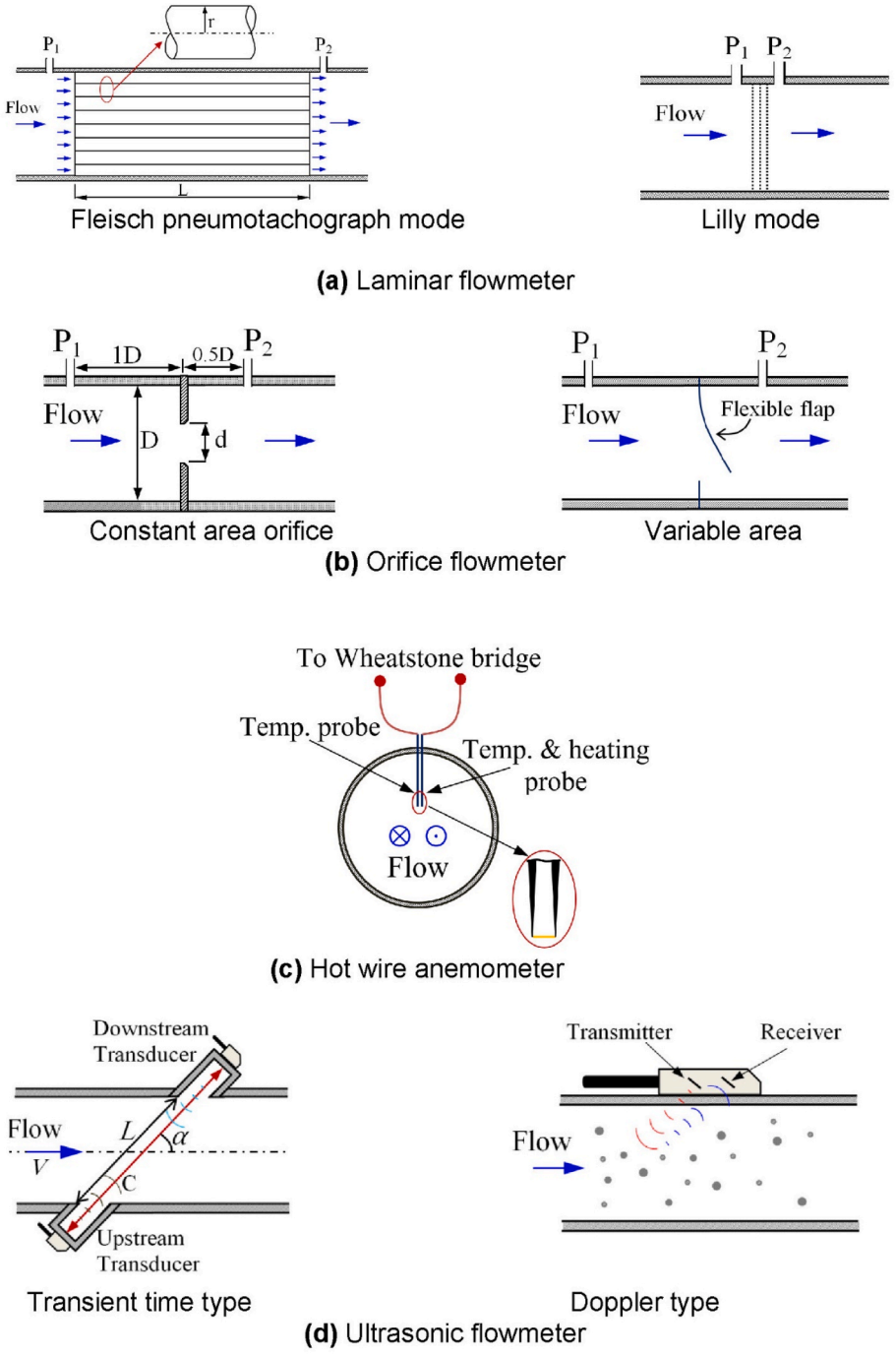

Fig. 1. Flowmeters used in ventilators.

As an alternative construction, several patents and papers have made the constriction as either a flexible tongue or flip-like plate [8–11]. This configuration (Fig. 1 (b)) provides the variable area with the flow to automatically adjust the area and hence compensates the successive increase in the pressure drop and hence minimizes the non-linearity of the instrument.

1.3. Hot wire anemometer

This type uses the convective heat transfer exchanged between the fluid and heating element. From its Greek name "anemos" which means "wind", it is mainly implemented in gas flow measurement. It consists of two temperature probes inserted in the pipe (Fig. 1 (c)). One of them measures the fluid temperature while the other does two jobs; receives electrical power and converts it to heat and at the same time senses the varied temperature, i.e., it is electrical resistance. This electrical resistance works as a resistive temperature device (RTD) which shows a linear relationship between the temperature and the resistance when the element is made of tungsten or platinum or other materials and non-linear relation if the element is made of semiconductors. According to Newton's cooling law, the convective heat transfer coefficient depends on the temperature difference between the fluid and the heating element and on the fluid characteristics as well.

Hotwire anemometer is found in two modes: constant temperature and constant power anemometers. In the former mode, the heating element is kept at constant temperature by increasing the current with increased velocity (and vice versa). This mode is popular because of several advantages; linear relation between the supplied current and the fluid velocity, high-frequency response, current feedback, low electronic noise level and immunity from element burnout when fluid velocity suddenly drops. On the other hand, constant power mode does not have feedback and experience unstable zero error, low response, and limited temperature compensation.

In medical applications, hotwire anemometer is widely used because of its good linearity and ability of measure bidirectional airflow. Generally, when it's used in ventilators, it needs periodic calibration due to its influence on the composition of gases moreover, nitrogen oxides are released due to the existence of the heating element.

1.4. Ultrasonic flowmeter

This type of flowmeter depends on the shifted (or reflected) ultrasonic signals traveling in a moving fluid. Two configurations of such flowmeter exist: Doppler type and transient time type. The former consists of a single transducer that transmits an ultrasonic signal and receives it when it is reflected by the impurities carried by the fluid (bubbles for example) as shown in Fig. 1 (d). If the bubble moves with the same velocity of the fluid, hence the reflected signal carries rich information about the fluid velocity. The transient type consists of a pair of transducers, transmitter and receiver aligned in a line inclined by an angle α with the axis of flow as shown in Fig. 1 (d). The signal transmitted by the upstream transducer is accelerated by the flowing fluid thus it takes less time to be received by the downstream transducer. Contrarily, the signal transmitted by the downstream transducer takes more time due to the deceleration imparted by the flowing fluid.

Because of the necessity of using filters in ventilators, the Doppler mode may fail in sensing the flow rate, thus, the transient time mode is widely used instead [7]. The time-flight measurements show a linear relationship between the gas velocity and the time difference, but indeed this is no longer true because the speed of sound varies with the gas temperature, the specific heat ratio, and its composition. As such, a temperature correction task requires an additional temperature sensor which in turn raises the cost of such devices. This is the reason why this type of flowmeter is rarely implemented in ventilators.

1.5. Other flowmeters

Continued research related to biomedical measurements has emerged many novel ideas of airflow sensors. The fiber-optic-based flow sensor proposed by Battista et al. [12] was directed to neonatal ventilators; it is based on inserting an optical emitting fiber in the tip of a flexible cantilever. An array of photodiodes is placed to face the fiber-optical tip to sense the illumination pattern which varies with the position of the end tip of the cantilever. The cantilever deflects depending on the airflow rate. A sensor based on fiber-optic is generally manifested immunity to electromagnetic interfaces with no hazardous of using electricity and low power consumption. This flow sensor was developed to accommodate bi-directional flow [13].

In other flow sensor types, lift induced force is utilized to sense the airflow rate. In this type, two force sensors are bounded on each end of a thin plate. The thin plate is supported on a center beam. When the center beam is adjusted at an inclined angle, the thin plate acts as an airfoil, and hence drag and lift forces are induced. The two force sensors which are based on piezoresistive sensing measure the lift force. Such a configuration is nonlinear, and its sensitivity is higher for a higher airflow rate. Svedin et al. [14] incorporated hot chips in the lift-force flow sensor. Therefore, based on thermal airflow sensing, the low flow rates can be measured with higher sensitivity. As continuous development of flow sensors, attention focused on micromachined flow sensors based on lift-force and convective heat transfer as can be found in Silvestri and Schena [15] and Kuo et al. [16].

Very recently, Koutsis et al. [17] designed and fabricated a modified spirometer based on thermal effect. Their intention was to develop a low-cost, accurate and portable spirometer for the treatment of Pulmonary Function Diseases (PFTs) out of the hospitals. The modification was by ducting the thermal flow sensor inside bypass housing incorporated in the main channel. They used two housing configurations, inside and outside the main pipe. The housing was fabricated using 3D printed technology. With this design, they ensured the laminar flow affecting the thermal flow sensor.

According to the spreads of covid-19 worldwide, acquisition of ventilators had become a severe challenge [18] therefore, ventilators should be fabricated locally, quickly and cheaply. One of the main units in ventilators is the flow sensor, and based on the aforementioned review, a laminar flowmeter is selected to be incorporated in the built ventilator. The laminar flowmeter is easy in local manufacturing and needs fewer sensors like pressure sensor to sense the airflow rate and temperature sensor to control the heater which compensates the condensation of the humid air, especially in the expiration airway. Compared with other flow sensors, there is no need for transducers for transmitting and receiving sound signals as in ultrasonic flow senor, also no released nitrogen oxides are resulting from the heating element of the hotwire flow sensor. Moreover, the 3D printing of high precision enhances the possibility of manufacturing the capillary passages of such a flowmeter accurately. It is worth noting that the 3D printing technique has been used to fabricate a flow sensor for small animals' ventilators by Jawde et al. [19], but for human ventilators, the 3D printed technique has not been used.

2. Laminar flowmeter: closure definition

From the first glance, the laminar flowmeter looks analogue with the well-known Ohm's law in electricity that is the current (flow) is directly proportional with the potential difference (pressure difference). The proportionality constant in the laminar flowmeter is the inverse of the dynamic viscosity of the fluid. In practice, however, the relation of the laminar flowmeter cannot be approximated as purely linear as Ohm's law. This is because variations of pressure through variable area passages can also create pressure drops. When variation of the area occurs abruptly, the generated pressure drop is significant and cannot be ignored. At the inlet and outlet of the capillary tubes, the area changes

abruptly generating such pressure drops.

Fluid flowing through individual capillary tubes experiences a developing boundary layer for a specified distance from entry. This distance is called "entrance length". The entrance length depends on the size of the capillary tube and the Reynolds number. Beyond this length, the boundary layer retains and the velocity profile is fixed also. The interesting matter is that at the inlet and outlet chambers, where the pressure taps are installed (Fig. 2 (a)), and within the entrance length the pressure drop is proportional with a density of fluid times the square of velocity [20]. Hence, the non-laminar pressure drops become significant at high flow rates and leading to high nonlinearity of the laminar flowmeter. To illustrate the mathematical description of circular capillary tubes, the Hagen-Poiseuille equation can be utilized to interpret the pressure drop in a straight pipe of length L and radius r as follow [21].

$$\Delta P = \frac{8\mu L}{\pi r^4} Q \tag{1}$$

where ΔP is the pressure drop across the tube, Q is the flow rate and μ is the dynamic viscosity.

Hagen-Poiseuille equation was derived for circular pipe by assuming incompressible flow with ignored gravity and purely axial flow with azimuthal symmetry. No-slip boundary condition is also applied on the wall.

Laminar or viscous flowmeter consists of n capillary tubes and the pressure drop across them is sensed by two taps placed at a distance from the entry and outlet of the capillary tubes. Thus, the effect of abrupt area changes is sensed by the pressure taps which in turn increase the nonlinearity between the pressure drop and the flow rate. As such, the non-linear relation of the laminar flowmeter can be written as [22]:

$$\Delta P = \frac{8\mu L}{n\pi r^4} Q + K_{losses}\rho Q^2 \tag{2}$$

where ρ is the fluid density.

In another way, capillary passages can be obtained by rolling up a thin metal sheet welded on it a corrugated another thin sheet. In nominal designs, the flat and corrugated sheets have the same thickness of 0.05 mm [23] as shown in Fig. 2 (b). Generally, the pressure drop in a non-circular laminar flowmeter can be written as:

$$\Delta P = K_{laminar}\mu Q + K_{losses}\rho Q^2 \tag{3}$$

In both equations (2) and (3), the coefficient K_{losses} involves three coefficients denoting the aforementioned three types of losses [2] namely, inlet, outlet and transition from developing to fully developed boundary layer.

$$K_{losses} = K_{inlet} + K_{transition} + K_{oulet} \tag{4}$$

where the subscripts the *inlet*, *outlet* and *transition* refer to; sudden contraction of the area at inlet; sudden expansion of the area at the outlet; and entrance length where the boundary layer is developing.

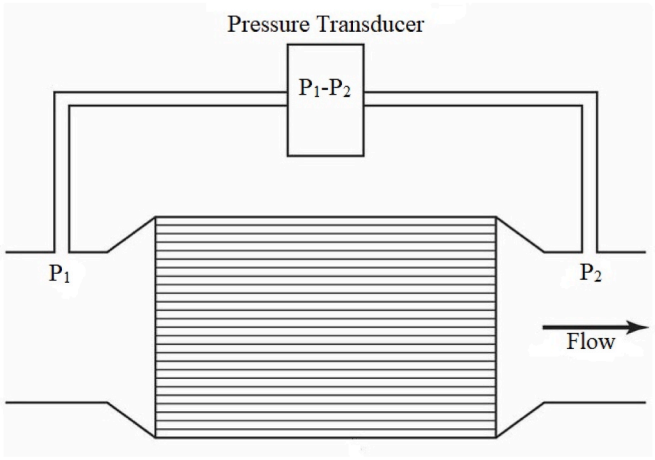

(a)

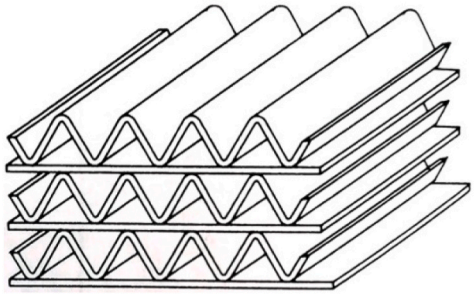

(b)

Fig. 2. (a) Laminar flowmeter with circular capillary tubes (b) Section of capillary corrugated passages before rolling up.

3. Fabrication and calibration

At the beginning of the covid-19 pandemic and in order to equip the locally manufactured ventilators with the necessary flow sensors, our team had decided to fabricate the sensor as quickly as possible. For this sake, we have focused our attention on the laminar flowmeter (LM) as it meets the demand of the emergency. Several models of LM's have been manufactured and tested until a suitable design is attained.

The first manufactured configuration was a bundle of 23 capillary tubes (2 mm diameter and 55 mm long) which have been inserted in 12.5 mm inner diameter tube and 19 mm outer diameter. Two 5 mm-diameter pressure taps had been drilled at distances 5 mm upstream and downstream of the capillary tubes bundle (as shown in Fig. 3 (a)). The model is tested in the calibration rig shown in Fig. 4 which is real simulation of the respiratory systems composed of inspiration and expiration-controlled periods. A HALOSCALE respirometer is connected to predict the total volume of flow and a stopwatch to calculate the volume flow rate. The calibration test of this model had shown unavoidable nonlinearity error and poor sensitivity to very low flow rates. Poor sensitivity means very low-pressure difference which falls below the least significant bit of the analogue to digital convertor (ADC) implemented in the ventilator. The second attempt was by using FDM 3D printer which has been implemented in printing only the main tube and its two taps, then the same type of capillary tubes used in the first attempt was inserted inside. The printed inner diameter of the main tube was 19.5 mm; thus, the number of capillary tubes was limited to 13 only. Again, we faced high nonlinearity and poor sensitivity. As such, the decision of using a more precise 3D printer was matured. SLS UV 3D printer was used then in fabricating the laminar flowmeter with more flexibility. The used 3D printer has (2560 × 1440) DPI with a resolution that reaches 25 μm layer thickness. The first product was that shown in Fig, 3 (c), where the entire flowmeter had been fabricated using this printer. Except for the number of capillary tubes, all dimensions are the same as those of Model 2 (Fig. 3 (b)), where 16 capillary tubes of 1.8 mm diameter. Unfortunately, the relation between the pressure difference and the flow rate also experienced poor sensitivity at low flow rates.

Returning to the models above and calculating the Reynolds numbers for each, we found that for a maximum airflow rate of 1600 ml/s, the Reynolds numbers are 2933, 5200 and 4716 for models presented in Fig. 3 (a), (b) and (c), respectively. Hence, it is asserted that the

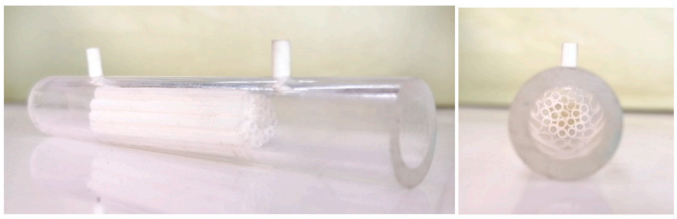

(a) LM with inserted capillary tubes, manually drilled pressure taps

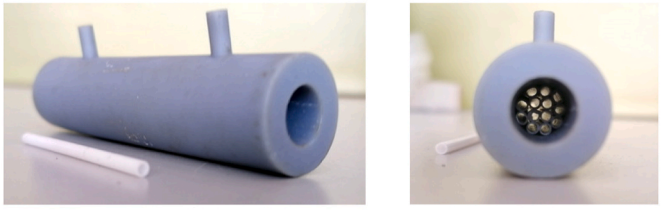

(b) LM with inserted capillary tubes, 3D printed pressure taps

(c) LM fully casted by high precision 3D printing, circular tubes and divergent pressure taps

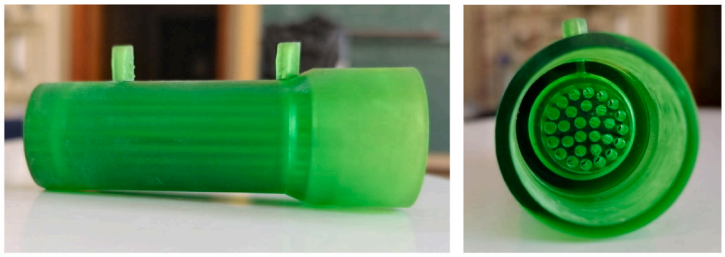

(d) LM fully casted by high precision 3D printing, circular tubes and approached pressure taps

Fig. 3. Various versions of manufacturing the LM flowmeter.

turbulent flow may be the cause of this nonlinearity and unstable sensitivity. To deal with this challenge, we decided to increase the number of capillary tubes. At the moment, we got feedback from clinical reports that the dimensions of the respiratory tubes set should be 22 mm outer diameter. As a result, we attained the configuration presented in Fig. 3 (d) which consists of 33 circular capillary tubes and gave a Reynolds number of 2286 at a maximum flow rate. The main adaptation of this model is displacing the pressure taps to be 5 mm from the upstream and downstream chambers as shown in Fig. 3 (f). In other words, this adaptation contributes to omitting the pressure losses arising from the abrupt area changes at the inlet and outlet, i.e., eliminating K_{inlet} and K_{outlet}. This approach was followed in various dispositions by Pena et al. [24].

The calibration test of model *d* is shown in Fig. 5 (a) which experiences some nonlinearity but better sensitivity. The best fit correlation is found to be agreed with Morgan Mercer Flodin (MMF) correlation [25].

$$Y = \frac{bK + Y_{lim}X^n}{K + X^n} \tag{5}$$

This correlation gave the best compromise between the accuracy and the zero intercept (the constant b) i.e. the flow rate is zero for zero pressure drop. A regression analysis of experimental data has achieved the coefficients of correlation (5) as:

$$Q = \frac{-7.986*42.6415 + 8455.275\Delta P^{0.7588}}{42.6415 + \Delta P^{0.7588}} \tag{6}$$

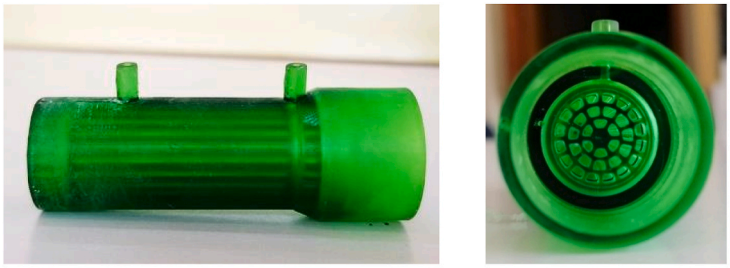

(e) LM fully casted by high precision 3D printing, non-circular tubes and approached pressure taps

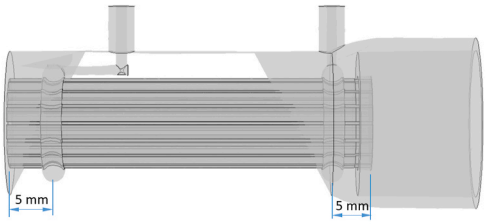

(f) Direct positioning of the pressure taps within the capillary tubes (approached pressure taps)

Fig. 3. (*continued*).

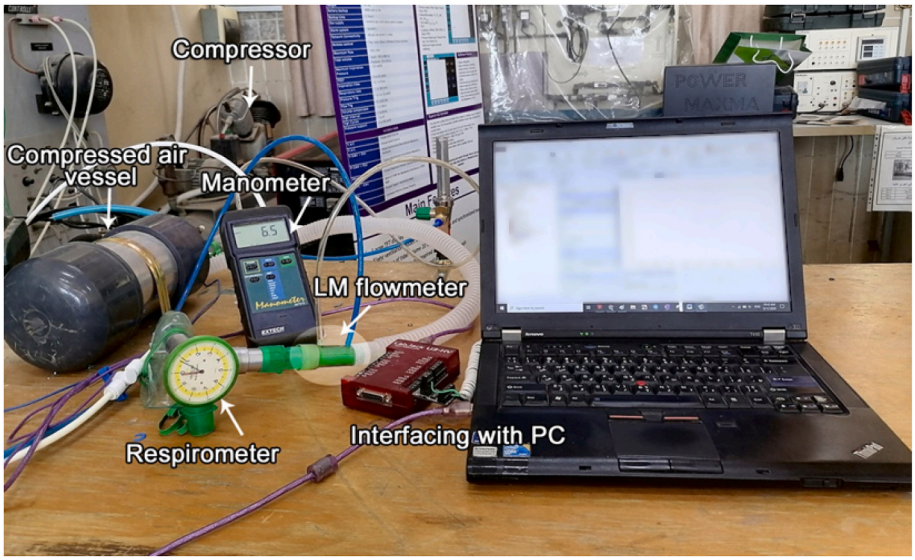

Fig. 4. Calibration flow rig.

With r-correlation factor = 0.99978 and standard error = 10.597. Fig. 5 (a) portrays also the correlation fit and the corresponding percentage error between them and the experimental data. The correlation experiences a maximum error of about 20% in a situation of a very low flowrate, while the average percentage error is 2.717%.

The flow sensor that should be inserted in the exhalation airway must have lowest resistant to the patient. We have found that capillary of circular sensor has relatively high pressure difference especially at high flow rates which is not acceptable clinically. As such, it is thought that there are some attempts to improve the flow sensor by making some modifications on the capillary tubes. We have made two modifications; the first is obstructing the central of the laminar flowmeter to diminish the effect of the maximum velocity at the tube center. The second modification was by making the cross-section of air passages trapezoidal. This configuration (Fig. 3 (e)) is easy in fabrication and centering and moreover, it serves in increasing the surface area and hence dominating the viscous effect where the principle of flowmeter relies on. The number of the trapezoidal capillary tubes is also 33 and the Reynolds number was found around 2000. The calibration curve (Fig. 5 (b)) shows different coefficients of the MMF correlation as:

$$Q = \frac{-5.5336*5.1213 + 3803\Delta P^{0.9957}}{5.1213 + \Delta P^{0.9957}} \tag{7}$$

with a better r-correlation factor of 0.99998 and a lower standard error

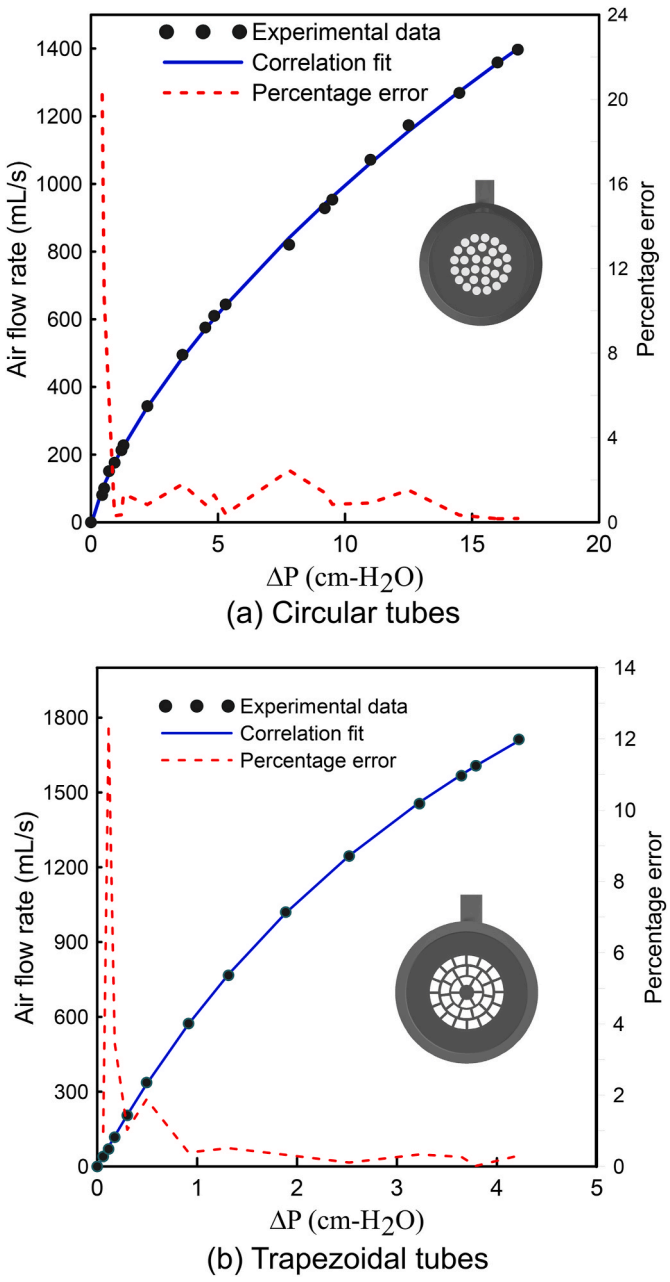

Fig. 5. Calibration of the 3D printed laminar flowmeter for (a) circular capillary tubes, "Model *d*" and (b) trapezoidal capillary tubes "Model *e*".

of 5.069. The recorded maximum percentage error in Fig. 5(b) is 12.28% while the average error is 1.68%, which indicates significant improvement. Moreover, the trapezoidal flow senor (Model e) demonstrates less pressure difference even for high flowrate. This object is very preferred because it produces less resistance to the patient during the inhalation and exhalation.

On the other hand, the zero errors appearing in relations (6) and (7) are recognized and accepted by providing the ventilator with an alarm of zero pressure difference, i.e. the correlation is already unused when the pressure difference is zero (actually no flow).

Regarding the correlations (6) and (7), the power (n) of the pressure difference was another objective of judgment between the circular and trapezoidal capillaries. The power of the pressure difference in relation (7) closes to unity ($n = 0.9957$), which reflects the bilinear relationship between the pressure difference and the airflow rate, and hence less nonlinear error.

Hagen-Poiseuille lines of models *d* and *e* are plotted in Fig. 6. For model *d*, the values of L, r, μ and n were set as 45 mm, 0.9 mm, 1.872×10^{-5} Pa s (at 30 °C) and 33, respectively. While for model e, the hydraulic diameter of the trapezoidal capillary passage was calculated to be 1.12 mm. Although these lines are theoretical, they emphasize the advantage of model *e* namely, the low pressure resistance even at a high flow rate.

As such, it is deduced that we have to adopt this final version (model *e*) to be included in the ventilator. However, this laminar flow sensor suffers from a condensation issue which requires an ancillary heating element. This is the sole limitation of this flow sensor. Eventually, it is important to highlight that we are planning to use two flow sensors in a clinical ventilator. One in inhalation port, which is installed inside the ventilator and the other in exhalation port, which is installed in such a way to enable easy replacement.

4. Conclusions

Coinciding with the attack of covid-19 pandemic, a volunteer team has decided to manufacture a ventilator under strict quarantine. This paper describes the stages of manufacturing the flowrate sensor in such a device. This sensor has been adopted after a review of the flowmeter types used in medical ventilators. The fabricated flow sensor was tested in the experimental rig with the aid of a HALOSCALE respirometer. The following remarks are concluded from this study.

1. It is possible to fabricate laminar flowmeters with high precisions using SLS UV 3D printers.
2. Positioning the pressure taps directly in the capillary tubes serves in eliminating the effect of abrupt changes between the capillary tubes and the inlet and outlet chambers. However, the transition losses cannot be eliminated because of the limited length of the flowmeter.
3. Different configurations of laminar flowmeters have been fabricated and tested. Built-in capillary passages of the trapezoidal cross-sectional area with directly positioned pressure taps showed the closest behavior to the linear Hagen-Poiseuille equation.
4. The main challenge in the laminar flowmeter is the condensation of the expiratory air. This task can be obviated by incorporating the flowmeter by an electrical heater, which needs extra elaboration.

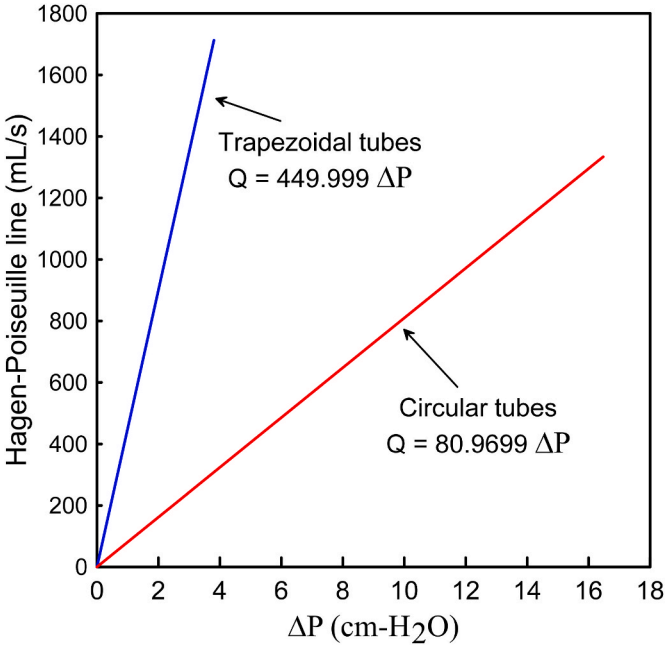

Fig. 6. Hagen-Poiseuille lines of circular and trapezoidal tubes.

Author statement

J. Alsalaet: Conceptualization, Methodology, Software., **B. Sh. Munahi:** Software, Data Curation, Writing- Original draft preparation. **R. Al-Sabur:** Visualization, Resources. **M. Al-Saad:** Visualization, Investigation. **A. K. Ali:** Conceptualization, Supervision. **Abdulbaseer Shari B:** Methodology, Investigation. **H. A. Fadhil:** Resources, Funding acquisition.**R. M. Laftah:** Resources. Project administration. **M. Ismael:** Formal analysis, Writing - Review & Editing.

Funding

None.

Declaration of competing interest

The authors declare that they have no known competing financial interests or personal relationships that could have appeared to influence the work reported in this paper.

References

[1] M.A. Warner, B. Patel, Mechanical ventilation, in Benumof and Hagberg's Airway Management 2013 Jan vol. 1 (pp. 981-997), WB Saunders.
[2] R.W. Miller, in: Flow Measurement Engineering Handbook, third ed., McGraw Hill, New York, 1996.
[3] S. Silvestri, The influence of flow rate on breathing circuit compliance and tidal volume delivered to patients in mechanical ventilation, Physiol. Meas. 27 (1) (2005) 23.
[4] J.C. Lilly, Flow meter for recording respiratory flow of human subjects, Methods Med. Res. 2 (1950) 113–121.
[5] R.J. Shephard, Pneumotachographic measurement of breathing capacity, Thorax 10 (3) (1955) 258.
[6] M.B. Jaffe, Gas flow measurement. In Capnography 2011 Mar 17 (pp. 397-406). New York Cambridge University Press.
[7] E. Schena, C. Massaroni, P. Saccomandi, S. Cecchini, Flow measurement in mechanical ventilation: a review, Med. Eng. Phys. 37 (2015) 257–264.
[8] J.J. Osborn, Variable orifice gas flow sensing head, US Patent 4,83,245 issued on Apr. 11, 1978.
[9] D.W. Guillaume, M.G. Norton, D.F. De Vries, Variable orifice flow sensing apparatus, US Patent 4 (1991) 993, 269 issued on Feb. 19.
[10] J. Stupecky, Variable area obstruction gas flowmeter, US Patent 5,83,621 issued on Aug. 13, 1991.
[11] C.I. Ciobanu, SD. Chaffer, Variable orifice flow sensor, US Patent, 5,970,801 issued on Oct. 26, 1999.
[12] L. Battista, S.A. Sciuto, A. Scorza, An air flow sensor for neonatal mechanical ventilation applications based on a novel fiber-optic sensing technique, Rev. Sci. Instrum. 84 (3) (2013), 035005.
[13] L. Battista, A. Scorza, F. Botta, S.A. Sciuto, A novel fiber-optic measurement system for the evaluation of performances of neonatal pulmonary ventilators, Meas. Sci. Technol. 27 (2) (2016), 025704.
[14] N. Svedin, E. Kälvesten, G. Stemme, A lift force sensor with integrated hot-chips for wide range flow measurements, Sensor Actuator Phys. 109 (2003) 120–130.
[15] S. Silvestri, E. Schena, Micromachined flow sensors in biomedical applications, Micromachines 3.2 (2012) 225–243.
[16] J.T.W. Kuo, L. Yu, E. Meng, Micromachined thermal flow sensors—a review, Micromachines 3 (2012) 550–573.
[17] T. Koutsis, P. Pikasis, A. Psyrris, G. Kaltsas, A thermal flow sensor with a 3D printed housing for spirometry applications, Microelectron. Eng. 5 (2020) 111286.
[18] K. Iyengar, S. Bahl, R. Vaishya, A. Vaish, Challenges and solutions in meeting up the urgent requirement of ventilators for COVID-19 patients, Diabetes & Metabolic Syndrome: Clin. Res. Rev. 14 (2020) 499–501.
[19] S.B. Jawde, B.J. Smith, A. Sonnenberg, J.H. Bates, B. Suki, Design and nonlinear modeling of a sensitive sensor for the measurement of flow in mice, Physiol. Meas. 39 (7) (2018), 075002.
[20] D.F. Elger, J.A. Roberson, B.C. Williams, C.T. Crowe, Engineering Fluid Mechanics, Wiley, Hoboken (NJ), 2016.
[21] F.M. White, in: Fluid Mechanics, eighth ed., McGraw-Hill Higher Education, New York, 2011.
[22] R.C. Baker, in: Flow Measurement Handbook, first ed., Univ. Press, Cambridge, 2000.
[23] J.P. Zock, Linearity and frequency response of Fleisch type pneumotachometers, Pflügers Archiv 391 (1981) 345–352.
[24] F.L. Pena, A.D. Diaz, M.R. Lema, S.V. Rodriguez, A new approach to laminar flowmeters, Sensors 10 (2010) 10560–10570, https://doi.org/10.3390/s101210560.
[25] G.A. Seber, C.J. Wild, Nonlinear Regression. Hoboken, first ed., vol. 62, John Wiley & Sons, New Jersey, 2003, p. 340.